

Intervalley Scattering and Weak Localization in Si-based Two-Dimensional Structures

A. Yu. Kuntsevich^a, N. N. Klimov^b, S. A. Tarasenko^c, N. S. Averkiev^c,

V. M. Pudalov^a, H. Kojima^b, and M. E. Gershenson^b

^a *P. N. Lebedev Physics Institute, 119991 Moscow, Russia*

^b *Department of Physics and Astronomy, Rutgers University, New Jersey 08854, USA and*

^c *A. F. Ioffe Physico-Technical Institute, 194021 St. Petersburg, Russia*

(Dated: May 14, 2018)

We have measured the weak localization magnetoresistance in (001)-oriented Si MOS structures with a wide range of mobilities. For the quantitative analysis of the data, we have extended the theory of weak-localization corrections in the ballistic regime to the system with two equivalent valleys in electron spectrum. This theory describes the observed magnetoresistance and allows the extraction of the phase breaking time τ_φ and the intervalley scattering time τ_v . The temperature dependences $\tau_\varphi(T)$ for all studied structures are in good agreement with the theory of electron-electron interaction effects in two-dimensional systems. The intervalley scattering is elastic and rather strong: τ_v is typically only an order of magnitude greater than the transport time, τ . It is found that the intervalley scattering rate is temperature-independent and the ratio τ_v/τ decreases with increasing the electron density. These observations suggest that the roughness of the Si-SiO₂ interface plays the major role in intervalley scattering.

PACS numbers: 72.10.-d, 73.20.Fz, 73.40.Qv

I. INTRODUCTION

Two-dimensional semiconductor structures with a degenerate ground state attract a great deal of attention because of the richness of low-temperature transport and thermodynamic phenomena that are often absent in systems with a simple band structure. The energy spectrum of a two-dimensional electron system in the metal-oxide-semiconductor (MOS) structures grown on the (001)-oriented Si surface consists of six subbands (valleys). At low temperatures and low electron densities, only two of them are occupied (the other four valleys are considerably higher in energy) [1]. The low-energy valleys are almost equivalent: the valley splitting Δ_v caused by an asymmetry of the confining potential is typically negligible in comparison with the Fermi energy [1]. When the intervalley scattering is weak, the valley degeneracy strongly affects both electron-electron interaction and weak localization (WL) effects in the conductivity. In particular, the interaction effects in Si MOS structures are strongly amplified by the valley degeneracy [2]; this accounts for the anomalous “metallic” temperature dependence of the resistivity in high-mobility Si MOSFETs at intermediate temperatures [3, 4]. Accordingly, the intervalley scattering plays an important role in the low-temperature phenomena in Si MOS structures: it determines the low-temperature cut-off of the metallic-like transport and could also modify the 2D metal-insulator transition observed in these structures at low electron densities [5, 6]. However, to the best of our knowledge, there were no systematic studies of the intervalley scattering in Si MOS structures.

The measurements of weak localization corrections to the conductivity of two-valley systems allow one to study intervalley scattering. The effect of intervalley scattering on WL depends on the relationship between the interval-

ley scattering time, τ_v , and the time of dephasing of the electron wave function, τ_φ . For weak intervalley scattering ($\tau_v \gg \tau_\varphi$), two valleys are independent at the time scale τ_φ relevant to the diffusion regime of WL. It is therefore expected that the magnitude of the WL correction is doubled in comparison with its value in a system with strong intervalley scattering ($\tau_v \ll \tau_\varphi$); the latter correction is the same as in a single-valley system because the valleys are completely mixed at the τ_φ time scale.

In numerous measurements of the WL magnetoresistance in Si MOS structures [7, 8, 9, 10], the experimental data were fitted using the Hikami-Larkin-Nagaoka (HLN) theory [11]. Interestingly, the factor-of-two enhancement of the WL correction was never observed, indicating that intervalley scattering is rather strong. In order to extract the intervalley scattering time from the WL magnetoresistance, the measurements should be extended towards higher magnetic fields. However, the HLN theory, which is used for fitting the WL magnetoresistance, was developed within the diffusive approximation (i.e. small magnetic fields, see below). Therefore, for an adequate description of the effect of intervalley scattering on WL in Si MOS structures, a theory applicable over a wider range of magnetic fields should be developed.

In this paper, we extend the ballistic (i.e. applicable to arbitrary classically-weak magnetic fields) theory of WL corrections to the case of two degenerate valleys. This enables the detailed quantitative analysis of the WL magnetoresistance measured for several Si MOS structures with the electron mobility varying over an order of magnitude. Rather small extracted values of τ_v ($\sim 10\tau$) indicate that the intervalley scattering in Si MOS structures is strong. We have found that (i) intervalley scattering is temperature-independent, i.e. elastic, (ii) the scattering rate depends monotonically on the electron density, and (iii) there is no simple correlation between the inter-

valley scattering and the mobility for different samples. The phase relaxation time in all studied structures is well described by the theory of electron-electron interaction effects [12].

The paper is organized as follows. In section II we describe the samples, measurement techniques and provide examples of experimental data. In section III, to compare our data with previously reported results, we fit the WL magnetoresistance with the HLN theory. The results of this analysis indicate that the WL correction is approximately a factor of 2 smaller than one could expect for a system with two independent valleys. The theory of the WL magnetoconductance for systems with degenerate multi-valley spectrum is presented in section IV and the data are analyzed using this theory in section V. In section VI we discuss the results of the data analysis, in particular, the intervalley and phase breaking times.

II. EXPERIMENT

Below we present data for three representative Si MOS-FET samples: (i) high-mobility ($\mu \approx 2 \text{ m}^2/\text{Vs}$ at 0.1 K) sample Si6-14 [4] which demonstrates a strongly pronounced “metallic-like” dependence $\sigma(T)$ and a metal-insulator transition with decreasing electron density n , (ii) sample Si39 with an intermediate mobility $\mu \approx 0.45 \text{ m}^2/\text{Vs}$ [13], and (iii) low-mobility sample Si40 with $\mu \approx 0.18 \text{ m}^2/\text{Vs}$ at $T < 4.2 \text{ K}$. The transport times for these samples within the studied range of n were $\tau \approx 2 \text{ ps}$, 0.6 ps , and 0.2 ps , respectively. The resistance was measured using the standard four-terminal AC technique by a resistance bridge LR700 (for sample Si6-14) and by SR830 lock-in amplifier in combination with a differential preamplifier (for samples Si39 and Si40). A sufficiently small measuring current (1-3 nA for Si6-14 and 50-100 nA for Si39 and Si40) was chosen to avoid overheating of electrons. The electron density, controlled by the gate voltage, was found from the period of the Shubnikov-de Haas oscillations and the dependence of the Hall resistance on magnetic field. Both results were consistent with each other within 2% accuracy in the studied range of densities; this uncertainty of n is insignificant for the further analysis. To ensure that only the lowest size quantization subband is filled [1], we performed measurements at $n < 4 \times 10^{12} \text{ cm}^{-2}$.

The WL magnetoresistance was measured at $T = 0.05 - 0.6 \text{ K}$ for high-mobility sample Si6-14, and at $T = 1.3 - 4.2 \text{ K}$ for samples Si39 and Si40. At these temperatures, the phase breaking time exceeds the transport time by one to two orders of magnitude. The magnetic field aligned perpendicular to the plane of Si MOS structures was varied from -1 to +1 kG (Si6-14) and from -3 to +3 kG (Si39 and Si40). When sample Si6-14 was measured at $T < 1 \text{ K}$, an additional in-plane field $\sim 200 \text{ G}$ was applied to quench the superconductivity in the current/voltage contact pads and the gate electrode made of

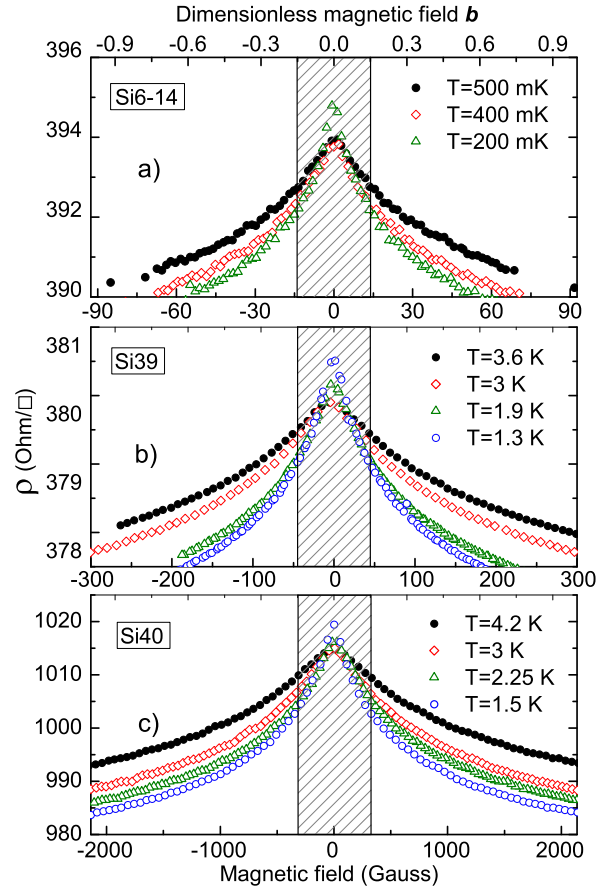


FIG. 1: Examples of the magnetoresistance $\rho(B)$ data for Si6-14, $n = 1 \times 10^{12} \text{ cm}^{-2}$ (a), Si39, $n = 3.6 \times 10^{12} \text{ cm}^{-2}$ (b), and Si40, $n = 3.5 \times 10^{12} \text{ cm}^{-2}$ (c). The data within the hatched regions have been used to extract the τ_φ value. Upper axes show the magnetic field in units of $B_{tr} = \Phi_0/2\pi l^2$, lower axes show the field in Gauss. The data points were chopped for clarity.

thin aluminum film. For reliable extraction of the phase relaxation time τ_φ from the WL magnetoresistance, we have chosen a small field step size: 1 G for Si6-14 and 3 G for Si39 and Si40. The examples of magnetoresistance $\rho(B)$ data for Si6-14, Si39 and Si40 at a fixed density and various temperatures are shown in Figs. 1a, 1b and 1c, respectively. Hereafter throughout the paper we will use magnetoconductance (MC) $\Delta\sigma \equiv \rho(B)^{-1} - \rho(B=0)^{-1}$.

III. FITTING THE DATA WITH THE HIKAMI-LARKIN-NAGAOKA THEORY

It is a common practice to extract the phase breaking time from the WL magnetoconductance using the HLN

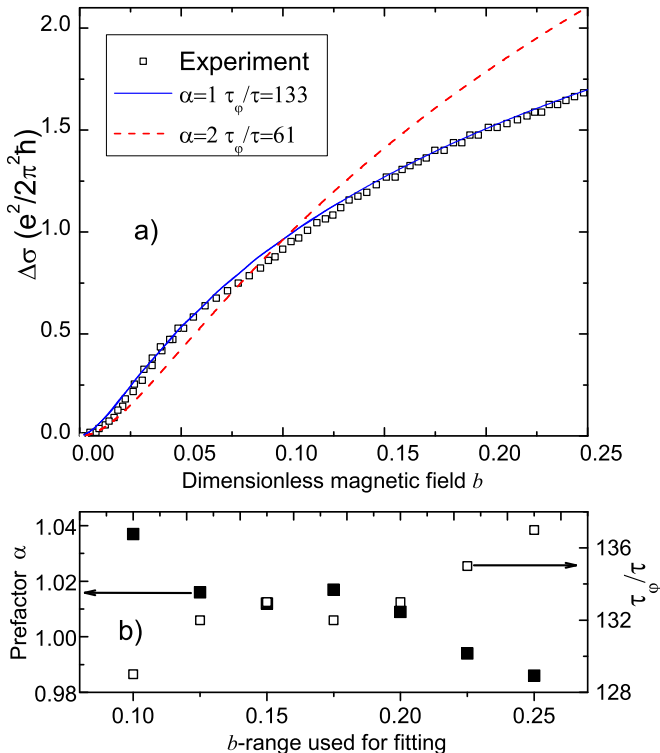


FIG. 2: a) Example of the MC data (points) for sample Si40, $T = 1.45K$ and $n = 3.34 \times 10^{12} \text{cm}^{-2}$. Solid line is calculated using Eq.(1) with two fitting parameters $\alpha = 1$ and $\tau_\varphi/\tau = 133$. The dashed curve is an attempt to fit the same data over the same range of b with a fixed prefactor $\alpha = 2$ and $\tau_\varphi/\tau = 61$. b) Dependences of the fitting parameters α (solid squares) and τ_φ/τ (open squares) on the magnetic field range $0 - b$ which was used for fitting.

theory[7, 8, 9, 10, 14]:

$$\Delta\sigma_{\text{HLN}}\left(b, \frac{\tau_\varphi}{\tau}\right) = \frac{\alpha e^2}{2\pi^2\hbar} \left[\psi\left(\frac{1}{2} + \frac{\tau}{b\tau_\varphi}\right) + \ln\frac{b\tau_\varphi}{\tau} \right]. \quad (1)$$

Here ψ is the digamma-function, e is the electron charge, \hbar is the Planck constant, $b = B/B_{tr}$ is the dimensionless magnetic field, $B_{tr} = \Phi_0/2\pi l^2$, $\Phi_0 = \pi\hbar/e$, and l is the transport mean free path [15]. The prefactor α and the dimensionless ratio τ_φ/τ are treated as fitting parameters. Note that with an increase of the magnetic field, the crossover from the diffusive regime ($b \ll 1$) to the ballistic regime ($b \sim 1$) is expected in the WL corrections. Equation (1) with prefactor $\alpha = 1$ is the exact result for a single-valley system in the diffusive regime, i.e. at $\tau_\varphi \gg \tau$ and for sufficiently small magnetic fields $b \ll 1$ [11]. On the other hand, the experimental data are often obtained beyond these limits and, therefore, should be described by more general ballistic theories [16, 17].

In Ref. [18], the HLN theory was numerically compared with the ballistic theory for a single-valley sys-

tem for various values of τ_φ/τ and magnetic fields b . It was found that both approaches agree with each other within a limited range of fields $b < 0.15$ provided that $\tau_\varphi/\tau > 30$ and the conductivity is much greater than $e^2/2\pi^2\hbar$. Thus, within these limits, Eq. (1) can be used for extraction of τ_φ from the WL magnetoresistance in a single-valley system, and the adjustable parameter α is approximately equal to 1. For a system with two valleys and weak intervalley scattering, the prefactor α is expected to be two times larger, because each valley contributes the term $\Delta\sigma_{\text{HLN}}$ with $\alpha \approx 1$ to $\Delta\sigma$.

Figure 2 a) shows a fit of our typical WL MC curve with Eq.(1). The fitting performed over the magnetic field range $b = 0 - 0.2$ gives $\tau_\varphi/\tau = 133$ and, contrary to the expectation for a two-valley system without intervalley scattering, $\alpha = 1$. Changing the magnetic field range, where the data are fitted, causes only minor variations of these parameters (see Fig. 2 b). An attempt to analyze the MC curve using Eq.(1) with a fixed prefactor $\alpha = 2$ results in a much worse fit (dashed line in Fig. 2 a).

Several reasons for the reduction of α in a single valley system have been considered in Ref. [14], including (i) Maki-Thompson correction, (ii) Density-of-states correction, (iii) higher order corrections in $(k_F l)^{-1}$, where k_F is the Fermi wave vector, and (iv) low τ_φ/τ ratio. The corrections (i) and (ii) were shown to be small [14]. To ensure that the higher order corrections are also small, we have studied the WL MC only for large conductances $\sim 100 \times e^2/2\pi^2\hbar$. When the ratio τ_φ/τ decreases, the HLN theory becomes inadequate, and the fitting procedure results in an artificially reduced prefactor. Correspondingly, we performed measurements at such low temperatures that the inequality $\tau_\varphi/\tau > 30$ was satisfied. We conclude therefore that the aforementioned reasons cannot account for a low value of the prefactor $\alpha \approx 1$ in the studied multi-valley structures. It should be noted that $\alpha \approx 1$ in Si MOS structures was obtained in numerous previous experiments [7, 8, 9, 10]. We show below that the prefactor reduction can be well described by the theory which explicitly takes the intervalley scattering into account.

IV. THEORY

A consistent theory of weak localization is developed in the framework of the diagram technique. The weak-localization corrections to the conductivity arise in the first order in the parameter $(k_F l)^{-1}$, where the mean free path l is governed by the scattering time τ , which is controlled by both *intra*-valley (τ_v) and *inter*-valley (τ_i) scattering processes:

$$1/\tau = 1/\tau_v + 1/\tau_i. \quad (2)$$

The weak-localization correction to the conductivity in the magnetic field has the form

$$\Delta\sigma(B) = \Delta\sigma^{(a)} + \Delta\sigma^{(b)}, \quad (3)$$

where the terms $\Delta\sigma^{(a)}$ and $\Delta\sigma^{(b)}$ correspond to the standard diagrams, which have been considered in detail in Refs. [17, 19, 20]. We neglect both valley and spin-orbit splitting in Si MOS structures. [21] Then, for the short-range scattering potential [22], one obtains

$$\Delta\sigma^{(a)} = \frac{\hbar}{\pi} \sum_{\alpha\beta} \int J_x^2(\boldsymbol{\rho}, \boldsymbol{\rho}') \mathcal{C}_{\beta\alpha}^{(3)\alpha\beta}(\boldsymbol{\rho}', \boldsymbol{\rho}) d\boldsymbol{\rho} d\boldsymbol{\rho}', \quad (4)$$

$$\Delta\sigma^{(b)} = \frac{\hbar}{\pi} \sum_{\alpha\beta\gamma\delta} \int J_x(\boldsymbol{\rho}, \boldsymbol{\rho}') J_x(\boldsymbol{\rho}'', \boldsymbol{\rho}) W_{\gamma\delta}^{\alpha\beta} \mathcal{C}_{\beta\gamma}^{(2)\delta\alpha}(\boldsymbol{\rho}', \boldsymbol{\rho}'') \times [G^R(\boldsymbol{\rho}, \boldsymbol{\rho}') G^R(\boldsymbol{\rho}'', \boldsymbol{\rho}) + G^A(\boldsymbol{\rho}, \boldsymbol{\rho}') G^A(\boldsymbol{\rho}'', \boldsymbol{\rho})] d\boldsymbol{\rho} d\boldsymbol{\rho}' d\boldsymbol{\rho}''.$$

Here $\alpha, \beta, \gamma, \delta = 1, 2$ are the valley indices; $J_x(\boldsymbol{\rho}, \boldsymbol{\rho}')$ is the x -component of the current vertex, which is defined as

$$\mathbf{J}(\boldsymbol{\rho}, \boldsymbol{\rho}') = ie \frac{k_F \tau}{m^*} \frac{\boldsymbol{\rho} - \boldsymbol{\rho}'}{|\boldsymbol{\rho} - \boldsymbol{\rho}'|} [G^A(\boldsymbol{\rho}, \boldsymbol{\rho}') + G^R(\boldsymbol{\rho}, \boldsymbol{\rho}')], \quad (5)$$

$G^A(\boldsymbol{\rho}, \boldsymbol{\rho}')$ and $G^R(\boldsymbol{\rho}, \boldsymbol{\rho}')$ are the advanced and retarded Green functions,

$$G^{R(A)}(\boldsymbol{\rho}, \boldsymbol{\rho}') = \sum_{s, k_y} \frac{\psi_{s, k_y}(\boldsymbol{\rho}) \psi_{s, k_y}^*(\boldsymbol{\rho}')}{E_F - E_s \pm i\hbar/(2\tau) \pm i\hbar/(2\tau_\varphi)}, \quad (6)$$

$\psi_{s, k_y}(\boldsymbol{\rho})$ is the wave function of an electron subject to an external magnetic field \mathbf{B} , which is perpendicular to the 2D plane, s and k_y are the quantum numbers (s is the Landau level number and k_y is the in-plane wave vector), $E_s = \hbar\omega_c(s + 1/2)$ is the energy of the s^{th} Landau level, $\omega_c = eB/m^*$ is the cyclotron frequency, m^* is the effective electron mass; $\mathcal{C}_{\gamma\delta}^{(2)\alpha\beta}(\boldsymbol{\rho}, \boldsymbol{\rho}')$ and $\mathcal{C}_{\gamma\delta}^{(3)\alpha\beta}(\boldsymbol{\rho}, \boldsymbol{\rho}')$ are the Cooperons which depend on four valley indices. The parameters $W_{\gamma\delta}^{\alpha\beta}$ are determined by intervalley and intravalley correlators of the scattering potential and are defined by

$$\langle V_{\alpha\mathbf{k}_1, \beta\mathbf{k}_2} V_{\gamma\mathbf{k}_3, \delta\mathbf{k}_4} \rangle N_{\text{imp}} = W_{\gamma\delta}^{\alpha\beta} \delta_{\mathbf{k}_1 + \mathbf{k}_3, \mathbf{k}_2 + \mathbf{k}_4}, \quad (7)$$

where $V_{\alpha\mathbf{k}_1, \beta\mathbf{k}_2}$ is the matrix element of scattering between electron states (β, \mathbf{k}_2) and (α, \mathbf{k}_1) in zero magnetic field, \mathbf{k}_j ($j = 1 \dots 4$) are wave vectors in the 2D plane, N_{imp} is the two-dimensional density of impurities, and the angle brackets stand for the averaging over impurity spatial distribution.

The Cooperons $\mathcal{C}_{\gamma\delta}^{(2)\alpha\beta}(\boldsymbol{\rho}, \boldsymbol{\rho}')$ and $\mathcal{C}_{\gamma\delta}^{(3)\alpha\beta}(\boldsymbol{\rho}, \boldsymbol{\rho}')$ represent the sums of internal parts of the fan diagrams starting with two and three lines, respectively, [17, 19, 20]. They can be found from the following equations:

$$\mathcal{C}_{\gamma\delta}^{(2)\alpha\beta}(\boldsymbol{\rho}, \boldsymbol{\rho}') = \sum_{\nu\mu} W_{\gamma\mu}^{\alpha\nu} W_{\mu\delta}^{\nu\beta} P(\boldsymbol{\rho}, \boldsymbol{\rho}') \quad (8)$$

$$+ \sum_{\nu\mu} W_{\gamma\mu}^{\alpha\nu} \int P(\boldsymbol{\rho}, \boldsymbol{\rho}'') \mathcal{C}_{\mu\delta}^{(2)\nu\beta}(\boldsymbol{\rho}'', \boldsymbol{\rho}') d\boldsymbol{\rho}'',$$

$$\mathcal{C}_{\gamma\delta}^{(3)\alpha\beta}(\boldsymbol{\rho}, \boldsymbol{\rho}') = \mathcal{C}_{\gamma\delta}^{(2)\alpha\beta}(\boldsymbol{\rho}, \boldsymbol{\rho}') - \sum_{\nu\mu} W_{\gamma\mu}^{\alpha\nu} W_{\mu\delta}^{\nu\beta} P(\boldsymbol{\rho}, \boldsymbol{\rho}'),$$

where $P(\boldsymbol{\rho}, \boldsymbol{\rho}') = G^A(\boldsymbol{\rho}, \boldsymbol{\rho}') G^R(\boldsymbol{\rho}, \boldsymbol{\rho}')$.

To calculate the weak-localization correction to the conductivity in multi-valley structures, we assume that the impurity potential is the same for particles in different valleys and, thus, the electron scattering in the valleys is strongly correlated. In particular, in the (001)-oriented Si-based structures the nonzero correlators are

$$W_{11}^{11} = W_{22}^{22} = W_{11}^{22} = W_{22}^{11}, \quad W_{12}^{21} = W_{21}^{12}. \quad (9)$$

Other correlators vanish due to averaging over the impurity positions because the lowest conduction-band valleys in silicon are located in the Δ -points of the Brillouin zone and, therefore, the Bloch functions contain oscillatory factors. We note that the intravalley and intervalley scattering times are determined by these correlators: $1/\tau_i = m^* W_{11}^{11}/\hbar^3$, $1/\tau_v = m^* W_{12}^{21}/\hbar^3$.

Using the standard procedure (see Refs. [19, 23]), one can expand $P(\boldsymbol{\rho}, \boldsymbol{\rho}')$ and the Cooperons in the series of eigenfunctions of a particle with the double charge in a magnetic field and derive equations for the weak-localization corrections $\Delta\sigma^{(a)}$ and $\Delta\sigma^{(b)}$. Calculations show that the corrections have the form

$$\Delta\sigma^{(a)} = -\frac{e^2 b}{2\pi^2 \hbar} \sum_{N=0}^{\infty} \mathcal{C}_N P_N^2, \quad (10)$$

$$\Delta\sigma^{(b)} = \frac{e^2 b}{2\pi^2 \hbar} \sum_{N=0}^{\infty} (\mathcal{C}_N + \mathcal{C}_{N+1}) Q_N^2 / 2. \quad (11)$$

$$\mathcal{C}_N = \frac{2(1 - \tau/\tau_v)^3 P_N}{1 - (1 - \tau/\tau_v) P_N} + \frac{P_N}{1 - P_N} - \frac{(1 - 2\tau/\tau_v)^3 P_N}{1 - (1 - 2\tau/\tau_v) P_N}, \quad (12)$$

where P_N and Q_N are coefficients which are given by

$$P_N = \sqrt{\frac{2}{b}} \int_0^{\infty} \exp \left[-x \sqrt{\frac{2}{b}} \left(1 + \frac{\tau}{\tau_\varphi} \right) - \frac{x^2}{2} \right] L_N(x^2) dx, \quad (13)$$

$$Q_N = \sqrt{\frac{2}{b}} \int_0^{\infty} \exp \left[-x \sqrt{\frac{2}{b}} \left(1 + \frac{\tau}{\tau_\varphi} \right) - \frac{x^2}{2} \right] \frac{L_N^1(x^2) x}{\sqrt{N+1}} dx,$$

and L_N and L_N^1 are the Laguerre polynomials.

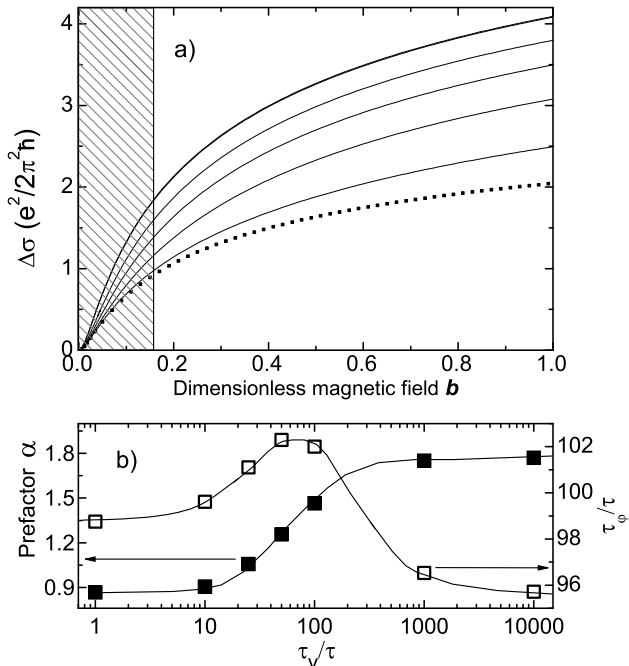


FIG. 3: a) WL magnetoconductance calculated for a two-valley system using Eqs. 3,10,11 (solid lines) and for a single-valley system [17] (dotted line). For solid curves from bottom to top, $\tau_v/\tau = 10, 25, 50, 100, 1000, 10000$, respectively. Two upper curves are indistinguishable by eye. For all the curves $\tau_\phi/\tau = 100$. The hatched region was used for fitting with Eq. (1). b) Dependences of the fitting parameters, α and τ_ϕ/τ , on τ_v/τ . The data points at $\tau_v/\tau = 1$ correspond to a single-valley system.

Equations (3), (10), and (11) describe the WL magnetoconductance over the whole range of classically weak magnetic fields $\omega_c\tau \equiv \mu B < 1$. In the limit of vanishing intervalley scattering ($1/\tau_v = 0$), Eqs. (10) and (11) are reduced to the conventional expressions for the WL corrections to the conductivity of a single-valley system [19] and, in particular, to the HLN formula [11] in the diffusion regime. The only difference is a prefactor of 2, which accounts for the valley degeneracy.

To illustrate the effect of intervalley scattering on the magnetoconductance, we calculated the $\Delta\sigma(b)$ dependence using Eqs. (3), (10), and (11) for a fixed $\tau_\phi/\tau = 100$ and various values of τ_v/τ . The results are shown in Fig. 3a by solid lines. For comparison, we also calculated the MC using a similar theory [17] developed for a single-valley system (dotted line). We then fitted these dependences over the range $b < 0.15$ using the HLN theory [Eq. (1)] with two fitting parameters, the prefactor α and τ_ϕ/τ . In other words, we fitted the theoretical curve the same way as the experimental data have been fitted above in Sec III.

Figure 3b shows the resultant fitting parameters; for

completeness, we also depicted α and τ_ϕ/τ for a single-valley system at $\tau_v/\tau = 1$. The main results of the fit are as follows: (i) the extracted phase breaking time τ_ϕ coincides with its true value within a few percent (this uncertainty is insignificant for further analysis), and (ii) the observed prefactor increases from ≈ 1 to ≈ 2 as τ_v increases and becomes greater than τ_ϕ . Therefore, the approximate equality $\alpha \approx 1$ is simply a consequence of a large ratio $\tau_\phi/\tau_v \gg 1$.

V. FITTING THE DATA WITH THE BALLISTIC THEORY

It is intuitively clear and will be discussed in more detail below, that the MC in low fields $b \ll 1$ is predominantly determined by τ_ϕ . In principle, one could use the “ballistic” theory for fitting the MC data in the whole range of magnetic fields and thus for determining both τ_ϕ and τ_v from a single fit. However the series Eqs. (10) and (11) converge very slowly in small b region. Therefore, to determine τ_ϕ , it is more practical to use in low fields Eq. (1), that was shown (see Fig. 3) to provide the correct τ_ϕ value.

Consequently, we have used the following procedure of extracting τ_v from the WL magnetoconductance. Firstly, we analyzed the MR data in sufficiently weak magnetic fields and at low temperatures. In this regime (the hatched regions in Fig. 1), the dephasing occurs at a time scale much greater than τ_v , and we can apply Eq. (1) for extracting τ_ϕ ; the second adjustable parameter, prefactor α , appears to be close to 1. At the next stage, we substitute τ_ϕ into the “ballistic” formulae [Eqs. (3), (10), (11)] and calculate the MC curves in a wide range of fields ($b < 1$) for various τ_v . Figure 4 illustrates this procedure using as an example the same MC data as in Fig. 2. We calculate $\Delta\sigma(b)$ using the summation technique similar to that described in Ref. [24] for single-valley systems.

Figure 4 shows that the experimental MC (circles) is smaller than the MC for a system with two unmixed degenerate valleys (curve 1) and larger than MC for a single valley system (curve 5). This observation again indicates that the MC in the studied Si MOS structures is affected by valley mixing. Curves 2, 3, and 4 in Fig. 4 correspond to $\tau_v/\tau = 15, 12,$ and 9 , respectively. Note that in the magnetic field range $b < 0.15$, these three curves, the experimental data, the HLN formula, and the ballistic result for a single valley system are almost indistinguishable from each other (see the inset to Fig. 4). Therefore, τ_v cannot be reliably found from the MC in low fields.

Figure 4 shows that the discrepancy between the curve 5 for a single-valley system and the curves 2,3,4 for two mixed valleys ($\tau_v/\tau = 15, 12,$ and 9) grows as b increases. This observation has a transparent physical explanation: with increasing b , the typical size of electron trajectories which contribute to the WL correction diminishes, and the valley mixing over the time of travel along these trajectories becomes small when $b > \Phi_0/D\tau_v$. As a result,

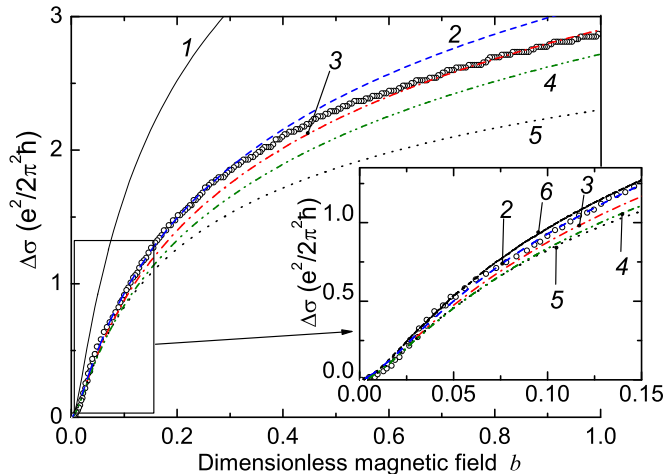


FIG. 4: Comparison between the WL magnetoresistance for sample Si40, $n = 33.4 \times 10^{11} \text{cm}^{-2}$, $T = 1.45 \text{K}$ and the ballistic theory. Different MC curves are calculated using Eqs. (3),(10),(11): 1 – for two unmixed valleys ($\tau_v = \infty$); 2 – $\tau_v/\tau = 15$; 3 – $\tau_v/\tau = 12$; 4 – $\tau_v/\tau = 9$; 5 – MC for a single-valley system (equal to curve 1 divided by 2). Inset blows up the data in the range $b < 0.15$. Curve 6 is the HLN theory (Eq. (1)) with a prefactor $\alpha = 1$ (see Fig. 2 a). $\tau_\varphi/\tau = 133$ for all calculated curves.

the WL magnetoconductance in strong magnetic fields approaches the theoretical prediction for a two-valley system with no intervalley scattering.

We also note that all calculated curves deviate from the experimental data. As Fig. 4 shows, curve 4 calculated for $\tau_v/\tau = 9$ at $b > 0.4$ is approximately parallel to but lower than the experimental data in magnetic fields $b > 0.4$. On the other hand, curve 2 calculated for $\tau_v/\tau = 15$ almost coincides with the data in low magnetic fields $b < 0.4$, though deviates substantially from them in higher fields. The minimal mean-square deviation of the calculated curve from the data is realized for $\tau_v/\tau = 12$ (curve 3).

Thus, the value of τ_v depends on the magnetic field interval (b_1, b_2) within which the MC data is fitted. The (τ_v/τ) values, obtained from fitting the difference $\Delta\sigma(b_1) - \Delta\sigma(b_2)$ as a function of (b_1, b_2) , decrease as $b = (b_1 + b_2)/2$ increases (see Fig. 5). This monotonic dependence has been reproduced for all samples and temperatures. We believe that this apparent $\tau_v(b)$ dependence is an artifact of the fitting procedure. In all above calculations we assumed τ_φ to be field-independent. However, τ_φ should depend on a perpendicular magnetic field [12]. To the best of our knowledge, there are neither experimental nor theoretical systematic studies of this dependence beyond the diffusive limit. Ignoring this dependence in our fitting could lead to the observed monotonic variation in τ_v with b .

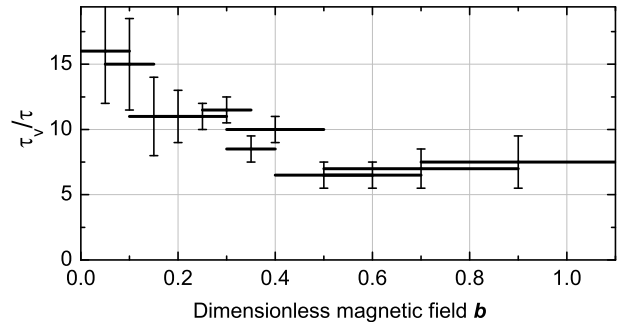


FIG. 5: Intervalley scattering time determined from fitting the difference, $\Delta\sigma(b_1) - \Delta\sigma(b_2)$, for the same magnetoresistance curve as in Fig. 4. The fitting ranges (b_1, b_2) are shown by the horizontal bars. $\tau_\varphi/\tau = 133$.

A question arises therefore what range of magnetic fields should be chosen for τ_v extraction? To answer this question we have analyzed errors of our method; the resulting root-mean-square sum of all errors is shown by the error bars in Fig. 5. The error analysis is presented in detail in the Appendix (Sec. IX), where it is shown that neither small fields ($b < 0.1$) nor large fields ($b \sim 1$) should be used for τ_v extraction. In weak fields, the MC is insensitive to τ_v , whereas in strong fields one approaches the limits of applicability of the theory developed in Sec. IV.

Therefore, we conclude that an intermediate range of magnetic fields is most suitable for extracting τ_v . For the further analysis, we choose the range $b = 0.2 - 0.4$. We have verified that our conclusions on the temperature and density dependences of τ_v are not affected if this range is changed.

VI. RESULTS AND DISCUSSION

A. Phase breaking time

As we have already mentioned, at the first stage of the analysis we estimated the phase breaking time τ_φ . Comparison of the $\tau_\varphi(T)$ dependences with the theory of interaction effects [12] is shown in Figs. 6 a-c. The uncertainty in the values of α and τ_φ (shown as the error bars in Fig. 6) reflects mainly the uncertainty in $\sigma(b)$ in the weak fields $b < 0.01$. The magnitude of the phase breaking time and its temperature dependence are in good agreement with the theory for all samples within the studied ranges of electron density [Si6-14: $n = (0.28 - 1.5) \times 10^{12} \text{cm}^{-2}$, Si39: $n = (2 - 2.5) \times 10^{12} \text{cm}^{-2}$, Si40: $n = (3 - 4) \times 10^{12} \text{cm}^{-2}$]. Note that no adjustable parameters are involved in this comparison,

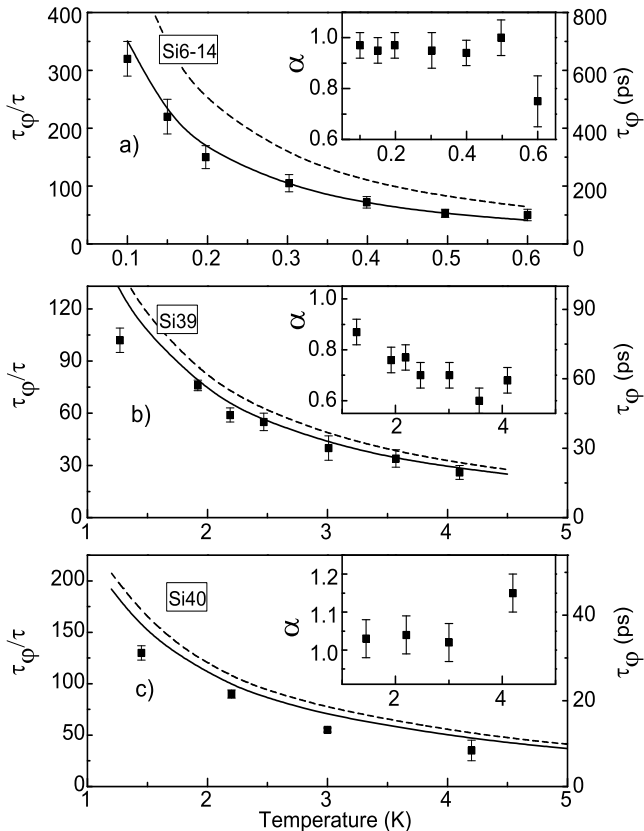


FIG. 6: Temperature dependence of the extracted τ_ϕ value in units of τ (left axes) and in picoseconds (right axes): a) Si6-14, $n = 9.98 \times 10^{11} \text{ cm}^{-2}$, b) Si39, $n = 29.4 \times 10^{11} \text{ cm}^{-2}$, c) Si40, $n = 33.4 \times 10^{11} \text{ cm}^{-2}$. Solid lines show the $\tau_\phi(T)$ dependence predicted by the theory of interaction corrections [12] with 15 triplet terms, dashed line - with 3 triplet terms. The insets show the corresponding temperature dependences of the prefactor α .

the Fermi-liquid parameter F_0^σ and the effective mass m^* were obtained in independent measurements [25].

The theoretical curves (solid lines in Fig. 6) are calculated following Ref. [12] for 15 triplet channels [2], which implies small valley splitting ($k_B T > \Delta_v$) and relatively weak intervalley scattering ($\hbar/\tau_v < k_B T$). As found from the analysis of the low-temperature transport and magnetotransport data [26], the condition $k_B T > \Delta_v$ was satisfied for samples Si6-14 and Si39 over the major part of the studied temperature range. Whether or not this condition is fulfilled for low mobility samples Si39 and Si40 is actually not important, because the measurements were performed at such high densities that the amplitude of the triplet term in the interaction corrections to τ_ϕ was small in comparison with the singlet term: changing the number of triplet terms from 15 (two-valley case) to 3 (single-valley case) caused variation of τ_ϕ by less than

5% (dashed line in Fig. 6). The condition $\hbar/\tau_v < k_B T$ is violated at temperatures lower than 0.3 K for sample Si6-14. Still, the $\tau_\phi(T)$ data agree better with theory when all 15 rather than 3 triplet terms are taken into account. The observed quantitative agreement of the experimental values of τ_ϕ with the theory suggests that τ_ϕ is weakly affected by intervalley scattering near the crossover $k_B T \tau_v / \hbar \sim 1$.

B. Prefactor α

By fitting the weak-field MC data with the HLN theory, we obtained the prefactor α that is close to 1 for all samples (see the insets to Fig. 6); this suggests that the valleys are intermixed on the τ_ϕ time scale. The decrease of α from 0.9 to 0.6 with increasing temperature, obtained for sample Si39 (see the inset to Fig. 6b), we believe, is an artifact, because relatively small values $\tau_\phi/\tau \sim 30$, observed for this sample at high temperatures, make Eq. (1) inadequate. The complete theory described in Sec. IV explains that small value of α is a consequence of a fast phase relaxation. For the same reason, there is a larger scattering in the values of $\alpha(T)$ for samples Si6-14 and Si40 at the highest temperatures (Fig. 6), where τ_ϕ is small.

It is worth noting that the smallness of prefactor α has been attributed to the intervalley scattering in Ref. [8]. However, the MC data in this experiment were fitted with the theory [23], which does not take into account the non-backscattering correction Eq. (11). Our estimates show that for the parameters of samples studied in Ref. [8] ($\tau_\phi/\tau = 20$, $\tau_v/\tau = 4$, and $b = 0.5-7$), the non-backscattering correction contributes about 50% to the extracted value of τ_v .

C. Intervalley scattering time: independence of temperature

Following the procedure described in Sec. V, we have extracted τ_v by fitting the WL MC data with “ballistic” Eqs. (3),(10),(11). Figure 7 shows that the values of τ_v are temperature-independent within the accuracy of our measurements. *This observation suggests that the intervalley scattering is elastic, i.e. governed by static disorder.* Similar conclusion can be also drawn from the fact that α remains close to 1, while the extracted τ_ϕ much exceeds τ_v and grows without saturation as T decreases (see Fig. 6). Indeed, were the intervalley scattering inelastic, one would have observed a prefactor $\alpha \sim 2$ because the dephasing would occur in two valleys independently and the intervalley scattering would be just an additional dephasing mechanism. In the latter case, a cut-off of the dephasing time at the level $\tau_\phi = \tau_v$ is also expected. The two observations, the absence of the cut-off and $\alpha \approx 1$ support the self-consistency of our analysis.

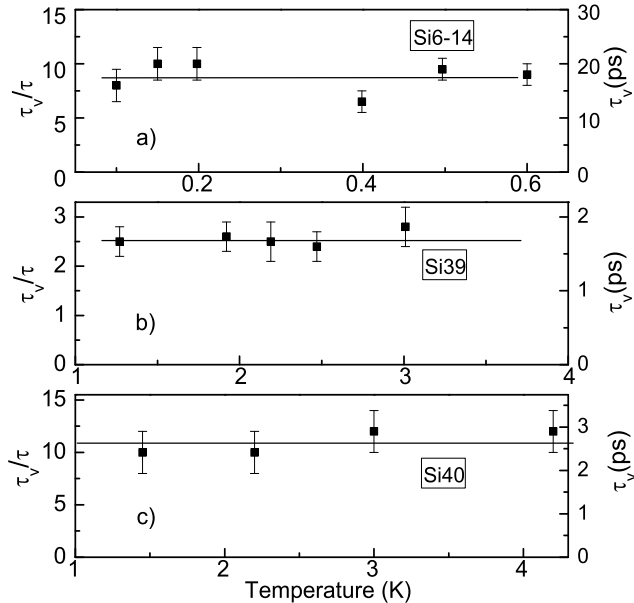


FIG. 7: Temperature dependence of τ_v in units of τ (left axes) and in picoseconds (right axes): a) Si6-14 $n=9.98 \times 10^{11} \text{ cm}^{-2}$, b) Si39 $n=29.4 \times 10^{11} \text{ cm}^{-2}$, c) Si40 $n=33.4 \times 10^{11} \text{ cm}^{-2}$. Solid horizontal lines show the average τ_v .

The intervalley transitions are not expected to be inelastic for the following reason. The intervalley scattering requires a large momentum transfer comparable to the vector of reciprocal lattice $2\pi/a \sim 10^8 \text{ cm}^{-1}$ (a is the interatomic distance). At liquid helium temperatures only static disorder can cause these transitions, as the momenta of electrons $k_F \sim 10^6 \text{ cm}^{-1}$ for the studied range of densities and phonons $k_{ph} \sim k_B T / (\hbar v_s)$ (here v_s is the sound velocity) are much smaller than $2\pi/a$. Static disorder can lead only to elastic scattering because it changes momentum of scattered electrons but does not change their energy.

D. Intervalley scattering time: density and sample dependence

Figure 8 shows the density dependence of τ_v values averaged over the temperature. For all three samples, the *relative* rate of the intervalley transitions (with respect to the momentum relaxation rate) increases with density. This points to the *dominant role of the Si-SiO₂ interface in the intervalley transitions*. The electron wave function Ψ in Si MOS structure is positioned mostly in the bulk silicon and exponentially decays in SiO₂ [1]. When the gate voltage (and, hence, the density n) is increased, the electrons are “pushed” towards the Si-SiO₂ interface, and the amplitude of the wavefunction at the interface, Ψ_0 , increases. The probability of the interface scattering is

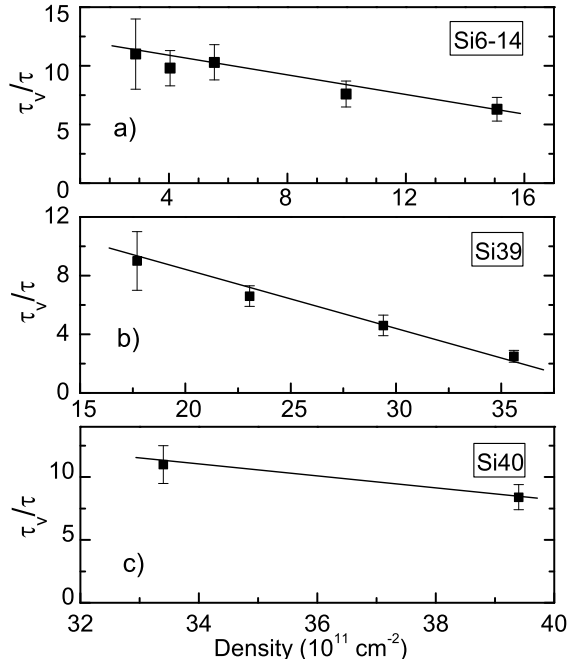


FIG. 8: Density dependence of the intervalley scattering time (averaged over temperature) for samples Si6-14 (a), Si39 (b) and Si40 (c).

proportional to $|\Psi_0|^2$ and increases with n [1]; this is in line with the behavior shown in Fig. 8.

In the experiments we used samples with the mobilities which vary over a decade. We find no correlation between τ_v and the mobility for different samples. This suggests that the intervalley scattering is determined by a sample-specific interface disorder, namely the surface roughness at the atomic length scale, which might be different for the samples fabricated on different wafers. In contrast to the intervalley scattering, the mobility is governed mostly by impurities in the bulk and by the interface roughness at a large length scale, $\sim 2\pi/k_F$.

The measured values of τ_v for all samples are within the interval $(3-12)\tau$, which indicates that the valley index remains a good quantum number at the time scale $\sim \tau$.

VII. SUMMARY

To summarize, we have studied the weak localization magnetoconductance in Si MOS structures over wide ranges of the electron densities, mobilities, and temperatures. In order to quantitatively analyze the experimental data, we have developed the theory of weak localization for two-dimensional multivalley systems, which is valid in both the diffusion and ballistic regimes. The theory, which explicitly takes the intervalley scattering into

account, allowed us to conduct the first detailed study of the intervalley scattering in the Si MOS structures. It was found that:

1. Intervalley scattering in Si MOS structures is an elastic and temperature-independent process.
2. The ratio τ_v/τ monotonically increases as the electron density decreases. This observation suggests that the intervalley scattering is governed by the disorder at the Si-SiO₂ interface.
3. There is no simple correlation between the intervalley scattering rate and the sample mobility (or the momentum relaxation rate); this points to a sample-specific rather than universal mechanism of the intervalley scattering.
4. The smallness of the prefactor $\alpha \sim 1$, that is obtained from fitting the experimental WL data with the HLN formula, is a consequence of a fast intervalley relaxation rate which exceeds the phase relaxation rate.
5. The temperature dependence of the phase relaxation time in Si MOS structures is in quantitative agreement with the theory of electron-electron interaction effects in disordered two-dimensional systems [12].

We note that the approach similar to that developed in this paper can be used for studies of intervalley relaxation in other multi-valley two-dimensional electron systems, such as AlAs-AlGaAs heterostructures [27], Si MOX structures [28], and Si-SiGe quantum wells [29].

VIII. ACKNOWLEDGEMENTS

The authors are thankful to I. V. Gornyi and G. M. Minkov for illuminating discussions. The research at Lebedev Institute and Ioffe Institute was supported by RFBR, INTAS, Programs of the RAS, Russian Ministry for Education and Science, Program “Leading scientific schools” (grants 5596.2006.2, 2693.2006.2, and the State contact 02.445.11.7346) and Russian Science Support Foundation. NK and MG acknowledge the NSF support under grant ECE-0608842. AK acknowledges Education and Research Center at Lebedev Physics Institute for partial support.

IX. APPENDIX: ANALYSIS OF POSSIBLE ERRORS IN τ_v

We present here an analysis of errors in the fitting procedure which determine the size of error bars in Fig. 5. As discussed in Section V, τ_v was found from the following equation:

$$\Delta\sigma(b_1)_{\text{EXP}} - \Delta\sigma(b_2)_{\text{EXP}} = \quad (14)$$

$$= \Delta\sigma(b_1, \tau_\varphi/\tau, \tau_v/\tau)_{\text{TH}} - \Delta\sigma(b_2, \tau_\varphi/\tau, \tau_v/\tau)_{\text{TH}}$$

Here subscript EXP denotes experimental data, subscript TH denotes calculation using Eqs. (3),(10),(11). Consequently, the uncertainty in τ_v is determined by (i) uncertainty in b , (ii) uncertainty in τ_φ and (iii) uncertainty in the conductivity. To estimate each contribution to the error, we varied the corresponding parameter (b , τ_φ or $\Delta\sigma$) within its uncertainty and determined the variation in τ_v by solving Eq. (14).

The uncertainty δb in $b = 2B\pi l^2/\Phi_0$ value is determined by the uncertainty in the mean free path l [15]. The latter is about 2-3 % due to the uncertainties in electron density n and Drude conductivity. However, δb affects τ_v rather weakly for the following reason: MC in the studied magnetic field range behaves approximately as $\ln(b)$, therefore $\Delta\sigma(b_1) - \Delta\sigma(b_2) \sim \ln(b_1/b_2) = \ln(B_1/B_2)$.

The error related to the uncertainty in τ_φ is essential in low magnetic fields where magnetoconductance is sensitive to τ_φ . Correspondingly, the error bars in low fields $b < 0.15$ in Fig. 5 are determined predominantly by the uncertainty in τ_φ .

Another source of errors is related to the precision of the absolute value of WL MC (“calibration error”). Indeed, the accuracy of our measurements of the absolute magnetoresistance value is $\sim 0.5\%$. Higher order corrections, Maki-Thompson and DOS corrections[14] can modify MC by approximately 2-3% (as shown in Ref. [14], $\delta(\Delta\sigma)/\Delta\sigma \approx 2e^2\rho_D/2\pi^2\hbar \approx 0.025$). In order to estimate this error we artificially changed our experimental data by 3% and studied the corresponding change in τ_v . The error appears to grow in small magnetic field where magnetoconductance is weakly sensitive to τ_v . Therefore, *small fields should not be used for the extraction of τ_v* . In large magnetic fields ($b \sim 1$) MC becomes again weakly sensitive to τ_v , and the latter error grows as b increases, as shown by the error bars in Fig. 5. The calibration error is minimal in intermediate magnetic fields, where MC is most sensitive to τ_v .

Our attempts to analyze the WL MC data in strong fields $b > 1$ using Eqs. (3),(10),(11) resulted in a large uncertainty of the fitting parameter τ_v/τ (large scattering of extracted τ_v/τ for various electron densities and temperatures). In large magnetic fields, there are several other error mechanisms which are difficult to take into account. For example, at $b \sim 1$, τ_φ differs from its small-field value [12]. Moreover, in Ref. [30] the MC for $b > 1$ was shown to behave in a non-universal manner: it strongly depends on details of scattering potential, whereas our theory assumes an uncorrelated short-range disorder. Some other mechanisms of magnetoconductance (such as classical memory effects, interaction corrections, Maki-Thompson corrections etc.) may also become essential in large fields where the shape of WL

MC curve flattens. Therefore we believe that the intermediate field range $b = 0.2 - 0.4$ is optimal for the

extraction of the intervalley scattering rate.

-
- [1] T. Ando, A. B. Fowler, and F. Stern, *Rev. Mod. Phys.* **54** (2) 437 (1982).
- [2] A. Punnoose and A. M. Finkel'stein, *Phys. Rev. Lett.* **88**, 016802 (2002).
- [3] G. Zala, B. N. Narozhny, and I. L. Aleiner, *Phys. Rev. B* **64**, 214204 (2001).
- [4] V. M. Pudalov, M.E.Gershenson, H. Kojima, G. Brunthaler, A. Prinz, and G. Bauer, *Phys. Rev. Lett.* **91**, 126403 (2003).
- [5] S. V. Kravchenko, G. V. Kravchenko, J. E. Furneaux, V. M. Pudalov, and M. D'Iorio, *Phys. Rev. B* **50** 8039 (1994).
- [6] Alexander Punnoose and Alexander M. Finkel'stein, *Science* **310**, 289 (2005).
- [7] R. G. Wheeler, *Phys. Rev. B* **24** 4645 (1981).
- [8] S. Kawaji and Y. Kawaguchi, *J. Phys. Soc. Jpn.* **53**,2868 (1984).
- [9] G. Brunthaler, A. Prinz, G. Bauer, and V. M. Pudalov, *Phys. Rev. Lett.* **87**, 096802 (2001).
- [10] M. Rahimi, S. Anissimova, M. R. Sakr, S. V. Kravchenko, and T. M. Klapwijk, *Phys. Rev. Lett.* **91**, 116402 (2003).
- [11] S. Hikami, A. Larkin, and Y. Nagaoka, *Progr. Theor. Phys.* **63**, 707 (1980).
- [12] G. Zala, B. N. Narozhny, and I. L. Aleiner, *Phys. Rev. B* **64**, 214204 (2001).
- [13] V. M. Pudalov, G. Brunthaler, A. Prinz, and G. Bauer, *Physica E* **3**, 79 (1998).
- [14] G. M. Minkov, A. V. Germanenko, and I. V. Gornyi, *Phys. Rev. B* **70**, 245423 (2004).
- [15] The transport mean free path l was determined from the formula $\sigma_D = (e^2/2\pi\hbar) \times k_F l \times n_v$, where $k_F = \sqrt{2\pi n/n_v}$, $n_v = 2$ for a two-valley system, σ_D is the Drude conductivity which for simplicity was taken equal to $\sigma(B=0)$; this simplification is justified for $\sigma \gg e^2/2\pi\hbar$.
- [16] H-P. Wittman and A. Schmidt, *Journal of Low Temperature Physics* **69**, 131 (1987).
- [17] A. P. Dmitriev, V. Yu. Kachorovskii, and I.V. Gornyi, *Phys. Rev. B* **56**, 9910 (1997).
- [18] G. M. Minkov, A. V. Germanenko, V. A. Larionova, S. A. Negashev, and I. V. Gornyi, *Phys. Rev. B* **61**, 13164 (2000).
- [19] V.M. Gasparian and A.Yu. Zyuzin, *Fiz. Tverd. Tela* **27**, 1662 (1985) [*Sov. Phys. Solid State* **27**, 1580 (1985)].
- [20] N. S. Averkiev, L. E. Golub, S. A. Tarasenko, and M. Willander *Phys. Rev. B* **64**, 045405 (2001).
- [21] We neglected spin-orbit splitting because no signatures of the antilocalization were seen in our Si-MOS structures down to the lowest temperatures. Our theory treats the valleys as equivalent, assuming $\Delta_v\tau/\hbar < 1$. As for the experimental data, from independent estimates [26] we have verified that the inequality $\Delta_v\tau/\hbar < 1$ is satisfied for all studied Si MOS structures. In general, depending on the valley splitting, the weak localization should be described either by the theory developed in the present paper ($\Delta_v\tau/\hbar < 1$) or the theory [20] ($\Delta_v\tau/\hbar \gg 1$).
- [22] As follows from our SdH measurements for all samples, as well as from numerous other experiments [1], the ratio of the large-angle scattering time τ to the quantum time (or any-angle scattering time) τ_q is close to unity in the studied range of electron densities. This result implies that the scattering in the studied samples is short-range.
- [23] A. Kawabata, *J. Phys. Soc. Jpn.* **53**, 3540 (1984).
- [24] S. McPhail, C. E. Yasin, A. R. Hamilton, M. Y. Simmons, E. H. Linfield, M. Pepper, and D. A. Ritchie, *Phys. Rev. B* **70**, 245311 (2004).
- [25] V. M. Pudalov, M. E. Gershenson, H. Kojima, N. Butch, E. M. Dizhur, G. Brunthaler, A. Prinz, and G. Bauer, *Phys. Rev. Lett.* **88**, 196404 (2002).
- [26] Δ_v was estimated from fitting the low-temperature $\sigma(T)$ data [4] with the theory of interaction corrections, where valley splitting was explicitly taken into account [see S. A. Vitkalov, K. James, B. N. Narozhny, M. P. Sarachik, T. M. Klapwijk, *Phys. Rev. B* **67**, 113310 (2003)]. For samples Si6-14 Δ_v was estimated to be less than 0.3 K, for Si39 - less than 2 K, and for Si40 - less than 6 K. Additionally, for all three samples, Δ_v was estimated from the absence of valley-related features (beats) in SdH oscillations of ρ_{xx} in weak magnetic fields (for Si6-14 Δ_v is less than 0.5 K, for Si39 - less than 2 K, for Si40 - less than 6 K).
- [27] K. Vakili, Y. P. Shkolnikov, E. Tutuc, E. P. De Poortere, and M. Shayegan, *Phys. Rev. Lett.* **92**, 186404 (2004).
- [28] K. Takashina, A. Fujiwara, S. Horiguchi, Y. Takahashi, and Y. Hirayama, *Phys. Rev. B* **69**, 161304(R) (2004)
- [29] K. Lai, T.M. Lu, W. Pan, D.C. Tsui, S. Lyon, J. Liu, Y.H. Xie, M. Muhlberger, and F. Schaffler, *Phys. Rev. B* **73**, 161301(R) (2006).
- [30] A. V. Germanenko, G. M. Minkov, A. A. Sherstobitov, and O. E. Rut, *Phys. Rev. B* **73**, 233301 (2006).